

## Hydrogen storage behaviours of nanocrystalline and amorphous $Mg_{20}Ni_{10-x}Co_x$ ( $x=0-4$ ) alloys prepared by melt spinning

ZHANG Yang-huan(张羊换)<sup>1,2</sup>, ZHAO Dong-liang(赵栋梁)<sup>1</sup>, LI Bao-wei(李保卫)<sup>2</sup>,  
QI Yan(祁焱)<sup>1</sup>, GUO Shi-hai(郭世海)<sup>1</sup>, WANG Xin-lin(王新林)<sup>1</sup>

1. Department of Functional Material Research, Central Iron and Steel Research Institute, Beijing 100081, China;
2. School of Material, Inner Mongolia University of Science and Technology, Baotou 014010, China

Received 2 March 2009; accepted 26 May 2009

**Abstract:** The  $Mg_2Ni$ -type alloys with nominal compositions of  $Mg_{20}Ni_{10-x}Co_x$  ( $x=0, 1, 2, 3, 4$ , %, mass fraction) were prepared by melt-spinning technology. The structures of the alloys were studied by XRD, SEM and HRTEM. The hydrogen absorption/desorption kinetics and the electrochemical performances of the alloys were measured. The results show that no amorphous phase forms in the as-spun Co-free alloy, but the as-spun alloys containing Co show a certain amount of amorphous phase. The hydrogen absorption capacities of the as-cast alloys first increase and then decrease with the incremental change of Co content. The hydrogen desorption capacities of as-cast and spun alloys rise with increasing Co content. The melt spinning significantly improves the hydrogenation and dehydrogenation capacities and kinetics of the alloys. The substitution of Co for Ni clearly enhances the discharge capacities of the alloys and the cycle stability of the as-spun alloys.

**Key words:**  $Mg_2Ni$ -type alloy; melt-spinning; structure; hydrogen storage behaviour

### 1 Introduction

Among the known alloys with a potential use in hydrogen storage, Mg and Mg-based metallic hydrides are considered to be more promising candidates because of their high hydrogen storage capacity and low price. Unfortunately, the practical applications are limited due to poor absorption/desorption kinetics and high thermodynamic stability of these kinds of metal hydrides. Therefore, finding ways of improving the hydration kinetics of Mg-based alloys has been one of the main challenges faced by researchers in this area. Various attempts, particularly mechanical alloying (MA)[1], surface modification[2] and alloying with other elements[3], have been undertaken to improve the activation and hydriding properties.

LEI et al[4] obtained improved discharge capacity of around 500 mA·h/g for  $Mg_2Ni$  alloys prepared by MA at a current density of 20 mA/g. IWAKURA et al[5] have also improved the discharge capacity of Mg-based alloy with graphite surface modification by mechanical

grinding (MG). After surface modification with Ni powder by ball milling, KOHNO et al[6] have obtained a large discharge capacity of 750 mA·h/g at a current density of 20 mA/g for modified  $Mg_2Ni$  alloys. However, MA Mg-based alloys showed extremely poor electrochemical cycle stability[7]. Alternatively, the melt-spinning technique is the most useful method to obtain an amorphous and/or nanocrystalline phase in the absence of disadvantages inherent from the MA process and is more suitable for mass-production of amorphous alloys. Some advantages of amorphous alloys, including high strength and toughness, excellent corrosion resistance, have been clarified by the researchers in this field[8].

It was also expected that amorphous alloys produced by melt-spinning could have excellent hydriding characteristics even at room temperature, similar to the alloys produced by the MA process. HUANG et al[9] found that amorphous and nanocrystalline Mg-based alloy ( $Mg_{60}Ni_{25}$ )<sub>90</sub>Nd<sub>10</sub> prepared by melt-spinning displayed the highest discharge capacity of 580 mA·h/g and the maximum

**Foundation item:** Project(2006AA05Z132) supported by the National High-tech Research and Development Program of China; Projects(50871050, 50701011) supported by the National Natural Science Foundation of China; Project(200711020703) supported by Natural Science Foundation of Inner Mongolia, China; Project(NJzy08071) supported by High Education Science Research Program of Inner Mongolia, China

**Corresponding author:** ZHANG Yang-huan; Tel: +86-10-62187570; E-mail: [zyh59@yahoo.com.cn](mailto:zyh59@yahoo.com.cn)  
DOI: 10.1016/S1003-6326(09)60154-0

hydrogen storage capacity of 4.2% (mass fraction).

In this work, the element Ni in  $Mg_{20}Ni_{10}$  alloy was partially substituted by Co in order to improve hydrogen storage properties of the  $Mg_2Ni$ -type alloys. The ternary  $Mg_2Ni$ -type nanocrystalline and amorphous  $Mg_{20}Ni_{10-x}Co_x$  ( $x=0-4$ , %, mass fraction) alloys were prepared by melt spinning and their hydrogen storage performances were examined in detail.

## 2 Experimental

The nominal compositions of the experimental alloys were  $Mg_{20}Ni_{10-x}Co_x$  ( $x=0, 1, 2, 3, 4$ , %, mass fraction). For convenience, the alloys were denoted with Co content as  $Co_0, Co_1, Co_2, Co_3$  and  $Co_4$ , respectively. The alloy ingots were prepared using a vacuum induction furnace in a helium atmosphere at a pressure of 0.04 MPa. Part of the as-cast alloys was re-melted and spun by melt-spinning with a rotating copper roller. The spun ribbons with width of about 5 mm and thickness of 20–30  $\mu m$  were obtained. The spinning rate was approximately expressed by the linear velocity of the copper roller because it is too difficult to measure a real spinning rate, i.e., cooling rate of the sample during spinning. The spinning rates used in the experiment were 15, 20, 25 and 30 m/s, respectively.

The phase structures of the as-cast and spun alloys were determined by XRD diffractometer (D/max/2400). The diffraction, with the experimental parameters of 160 mA, 40 kV and 10 ( $^\circ$ )/min, was performed with Cu  $K_{\alpha 1}$  radiation filtered by graphite. The morphologies of the as-cast alloys were examined by scanning electronic microscope (SEM) (Philips QUANTA 400). The thin film samples of the as-spun alloys were prepared for observing the morphology with high resolution transmission electronic microscope (HRTEM) (JEM-2100F, operated at 200 kV), and for determining the crystalline state of the samples with electron diffractometer (ED).

Thermal stability and crystallization of the as-spun alloys were studied by means of DSC instrument (STA449C), and the heating temperature and rate are 600  $^\circ C$  and 10  $^\circ C$ /min, respectively.

The hydrogen absorption and desorption kinetics of the as-cast and spun alloys were measured by an automatically controlled Sieverts apparatus. The hydrogen absorption was conducted at 1.5 MPa and the hydrogen desorption in vacuum ( $1 \times 10^{-4}$  MPa) at 200  $^\circ C$ .

The amorphous alloy ribbons were pulverized and then mixed with carbonyl nickel powder in a mass ratio of 1:4. The mixture was cold pressed at a pressure of 35 MPa into round electrode pellets of 15 mm in diameter and total mass of about 1 g. A tri-electrode open cell, consisting of a metal hydride electrode, a sintered

$NiOOH/Ni(OH)_2$  counter electrode and a Hg/HgO reference electrode, was used for testing the electrochemical characteristics of the experimental alloy electrodes. A 6 mol/L KOH solution was used as electrolyte. The voltage between the negative electrode and the reference electrode was defined as the discharge voltage. In every cycle, the alloy electrode was first charged at a current density of 20 mA/g, after resting for 15 min; then it was discharged at the same current density to cut-off voltage of  $-0.500$  V. The environment temperature of the measurement was kept at 30  $^\circ C$ .

## 3 Results and discussion

### 3.1 Microstructure characteristics

XRD patterns of the as-cast and spun alloys are shown in Fig.1. It can be clearly seen in Fig.1(a) that no amorphous phase is found in the as-spun  $Co_0$  alloy, but the as-spun  $Co_4$  alloy shows the presence of an amorphous phase, and amorphous degree of the alloys significantly increases with rising Co content. Therefore, it can be concluded that the substitution of Co for Ni enhances the glass forming ability of the  $Mg_2Ni$ -type alloy. The impactful role of Co substitution on the glass forming ability is mainly attributed to the fact that atomic radius of Co is larger than that of Ni. The glass forming ability of the alloy is closely relevant to the difference of the atom radius of elements in the alloy. The larger the difference of the atom radius, the higher the glass forming ability of the alloy[10]. It can be seen in Fig.1(b) that the diffraction peaks of the  $Co_2$  alloy are obviously broadened with rising spinning rate, indicating the refinement of the grains and the increase of the stored stress in the grains. It can be derived by comparing Fig.1(a) with (b) that the substitution of Co for Ni does not change the major phase of the alloy, but it leads to the formation of secondary phase  $MgCo_2$ .

The SEM images of the as-cast  $Co_0$  and  $Co_4$  alloys are illustrated in Fig.2, showing that the substitution of Co for Ni causes the grains of the as-cast alloy to be significantly refined. The morphology of the alloy changes from bulky dendrite structure to massive structure. The result obtained by energy dispersive spectrometry (EDS) indicates that the major phase of the  $Co_0$  and  $Co_4$  alloys is  $Mg_2Ni$  (denoted as *A*), but Co substitution leads to the formation of the secondary phase  $MgCo_2$  (denoted as *B*), which is in agreement with the results of the XRD observation.

The morphologies of the as-spun (25 m/s)  $Co_0$  and  $Co_4$  alloys observed by HRTEM are shown in Fig.3, showing that the as-spun  $Co_0$  alloy displays a nanocrystalline structure with a grain size of about 30 nm, and its electron diffraction (ED) pattern appears in sharp multi-haloes, corresponding to a crystal structure. The

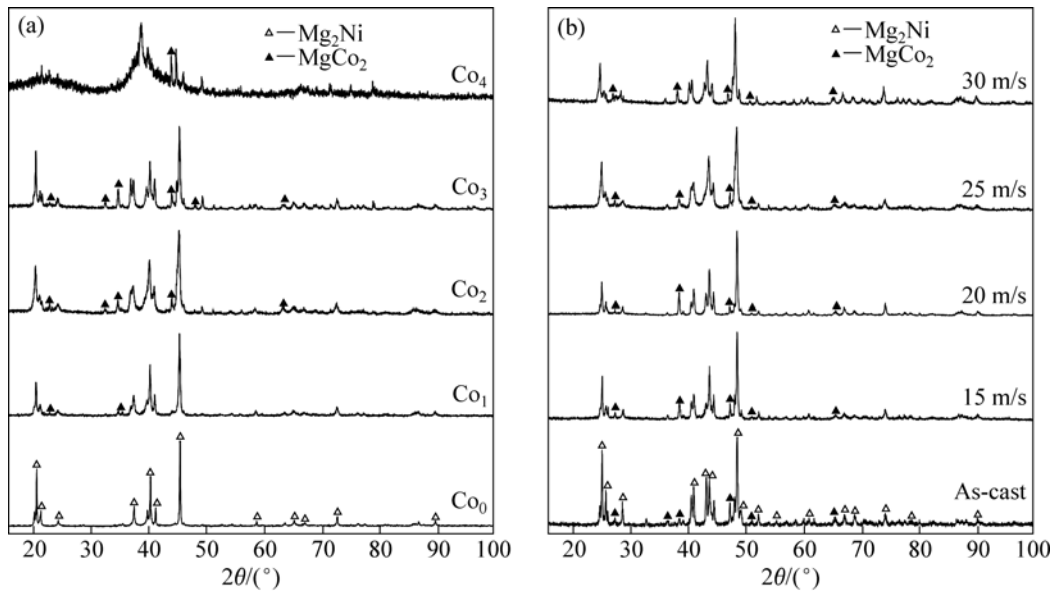


**Fig.1** XRD patterns of as-cast and spun  $Mg_{20}Ni_{10-x}Co_x$  alloys: (a) Effect of Co content with constant spinning rate of 25 m/s; (b) Effect of spinning rate with constant Co content of 2%

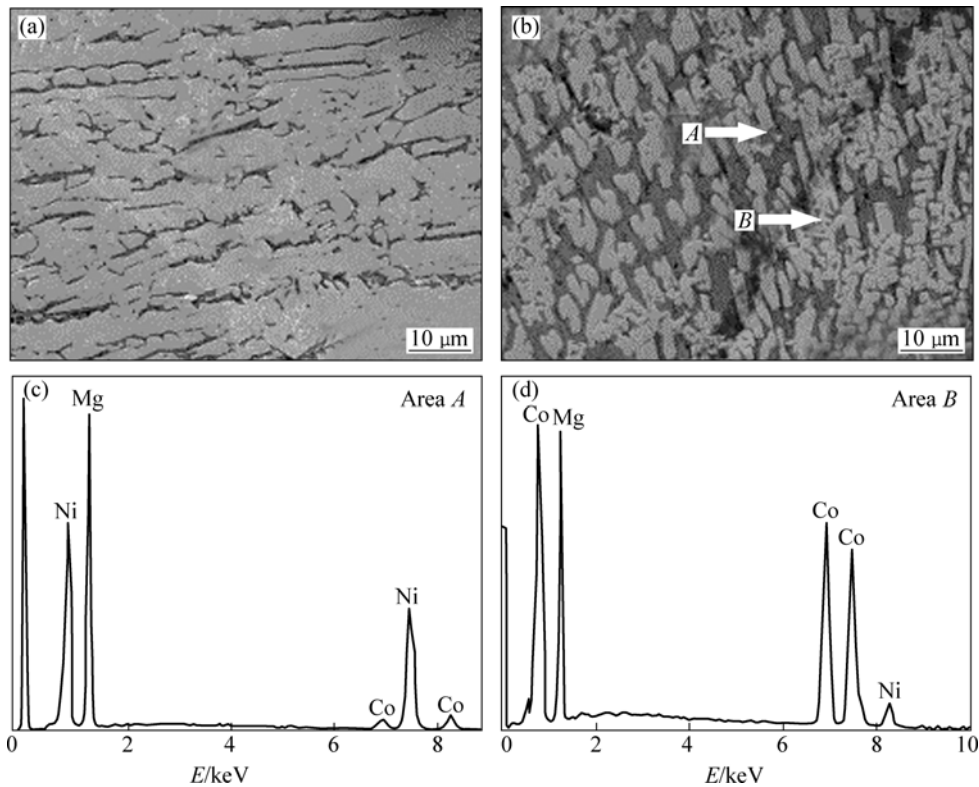


**Fig.2** SEM images ((a) and (b)) of  $Co_0$  and  $Co_4$  alloys together with typical EDS spectra ((c) and (d)) of areas *A* and *B* in Fig.2(b): (a) and (c)  $Co_0$  alloy; (b) and (d)  $Co_4$  alloy

morphologies of the as-spun  $Co_4$  alloy exhibit a feature of the nanocrystalline with a grain size of about 20 nm embedded in the amorphous matrix, and its electron diffraction pattern consists of broad and dull halo, confirming the presence of an amorphous structure. This result agrees very well with the XRD observation shown

in Fig.1.

### 3.2 Thermal stability and crystallization

In order to examine the thermal stability and the crystallization of the as-spun alloys, DSC analysis was conducted. The resulting profiles shown in Fig.4 reveal

that during heating the alloys crystallize completely, and the crystallization process of  $\text{Co}_4$  alloy consists of two steps. The first crystallization reaction at about  $232\text{ }^\circ\text{C}$  is connected with a sharp exothermic DSC peak, followed by a smaller and wider peak ( $418\text{ }^\circ\text{C}$ ) corresponding to a second crystallization reaction. It was proved that the first sharper peak corresponds to the crystallization (ordering) of the amorphous into nanocrystalline  $\text{Mg}_2\text{Ni}$ [11].

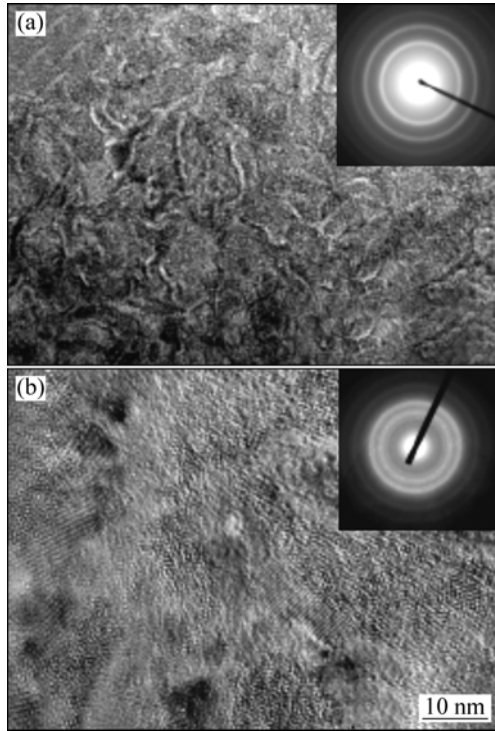


**Fig.3** Morphologies and ED of as-spun alloys (25 m/s) taken by HRTEM: (a)  $\text{Co}_0$  alloy; (b)  $\text{Co}_4$  alloy

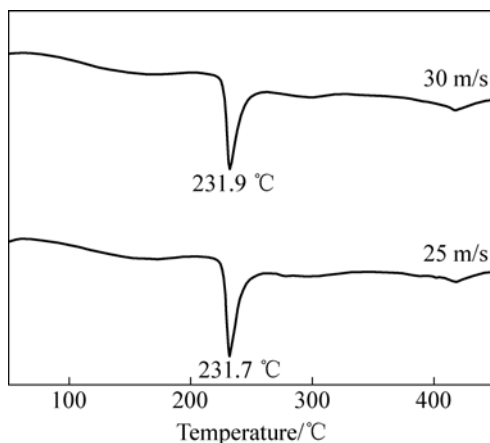


**Fig.4** DSC profiles of  $\text{Co}_4$  alloy spun at 25 and 30 m/s

### 3.3 Hydriding and dehydriding characteristics

The hydriding process was carried out under 1.5 MPa hydrogen pressure (in fact, this pressure is initial pressure of hydriding process) at  $200\text{ }^\circ\text{C}$ , and

dehydriding process was carried out in vacuum ( $1 \times 10^{-4}$  MPa) at  $200\text{ }^\circ\text{C}$ .

The hydrogen absorption kinetic curves of the as-cast and spun alloys are plotted in Fig.5, indicating that all the alloys show very fast hydrogen absorption rate and nearly reach their saturation capacities in 10 min. It can be seen in Fig.5(a) that the  $\text{Co}_4$  alloy displays the lower hydrogen absorption capacity for which the increased amount of secondary phase  $\text{MgCo}_2$  is mainly responsible because the hydrogen absorption ability of the  $\text{MgCo}_2$  phase is very poor. Fig.5(b) shows that the hydrogen absorption properties of the alloys are significantly improved by melt spinning. When the spinning rate is increased from 0 to 30 m/s, the hydrogen absorption capacity of the  $\text{Co}_2$  alloy in 10 min rises from 2.51% to 3.21%. The improved hydrogenation characteristics can be explained with the enhanced hydrogen diffusivity in the amorphous and nanocrystalline microstructures as the amorphous phase around the nanocrystalline leads to an easier access of hydrogen to the nano-grains, avoiding the long-range diffusion of hydrogen through an already formed hydride, which is often in the slowest stage of absorption.

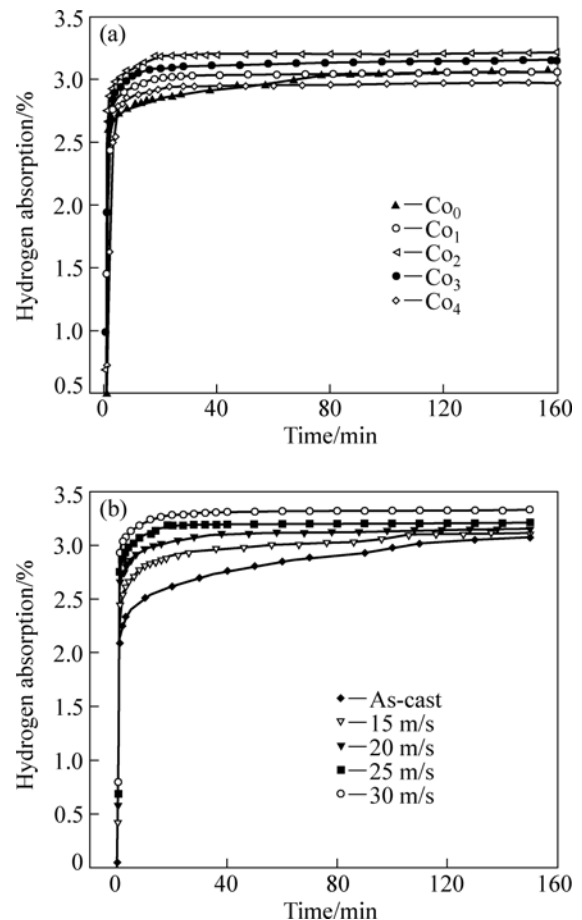


**Fig.5** Hydrogen absorption kinetic curves of as-cast and spun alloys: (a) Effect of Co content with constant spinning rate of 25 m/s; (b) Effect of spinning rate with constant Co content of 2%

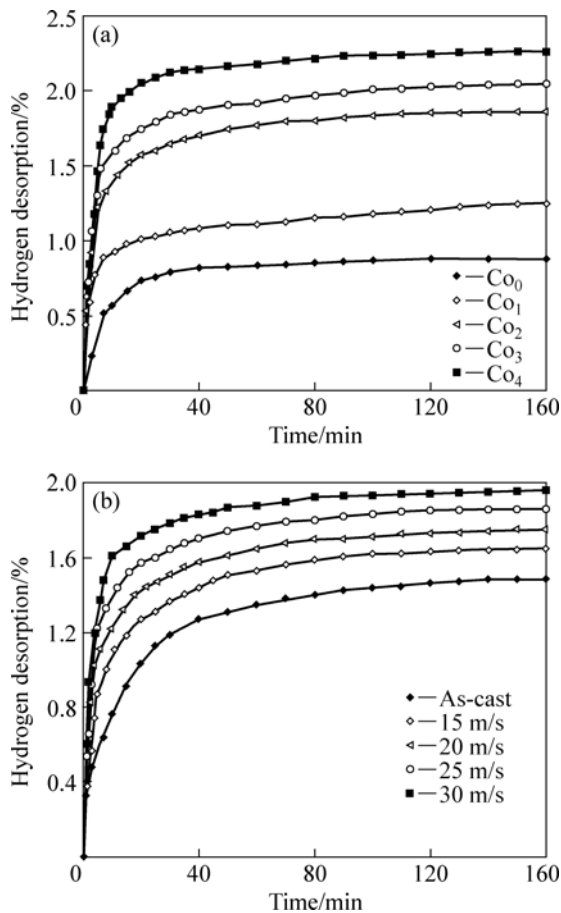
According to the result reported by ORIMO and FUJII[12], the distribution of the maximum hydrogen concentrations in three nanometer-scale regions, i.e. grain region and grain boundary region as well as amorphous region, have been experimentally determined to be 0.3% in the grain region of Mg<sub>2</sub>Ni, 4.0% in the grain boundary and 2.2% in the amorphous region. This reveals that the hydrides mainly exist in grain-boundary region and the amorphous phase region.

Fig.6 shows the hydrogen desorption kinetic curves of the as-cast and spun alloys. Fig.6(a) indicates that the Co substitution significantly improves the hydrogen desorption capacity and kinetics of the as-spun alloys. When Co content increases from 0 to 4%, the hydrogen desorption capacity of the as-spun (25 m/s) alloy in 10 min rises from 0.56% to 1.89%. It must be mentioned that the as-spun Co<sub>0</sub> alloy shows higher hydrogen absorption ability than Co<sub>4</sub> alloys (Fig.4), but its hydrogen desorption capability is the lowest. Therefore, it can be concluded that the substitution of Co for Ni improves the dehydrogenating performance of Mg<sub>2</sub>Ni-type alloy. Fig.6(b) shows that the dehydrogenation capability of the alloys is obviously meliorated with rising spinning

rate. When the spinning rate is enhanced from 0 to 30 m/s, the hydrogen desorption capacity of the Co<sub>2</sub> alloy in 10 min increases from 0.75% to 1.61%. The improved hydrogenation characteristics can be ascribed to two reasons. One is that Co substitution significantly intensifies the glass forming ability of Mg<sub>2</sub>Ni-type alloy because amorphous Mg<sub>2</sub>Ni shows an excellent hydrogen desorption capability. On the other hand, the substitution of Co for Ni in Mg<sub>2</sub>Ni compound decreases the stability of the hydride and makes the desorption reaction easier[13–14].

### 3.4 Electrochemical performances

The discharge capacity dependent on the cycle number of the alloys is illustrated in Fig.7, with the charging-discharging current density being 20 mA/g. It is shown that all the alloys have an excellent activation capability and attain their maximum discharge capacities at first charging-discharging cycle. It can be seen in Fig.7(a) that the discharge capacity of the as-spun alloys increases with rising Co content. When Co content increases from 0 to 4%, the discharge capacity of the as-spun (25 m/s) alloy rises from 113.6 to 376 mA·h/g.



**Fig.6** Hydrogen desorption kinetic curves of as-cast and spun alloys: (a) Effect of Co content with constant spinning rate of 25 m/s; (b) Effect of spinning rate with constant Co content of 2%

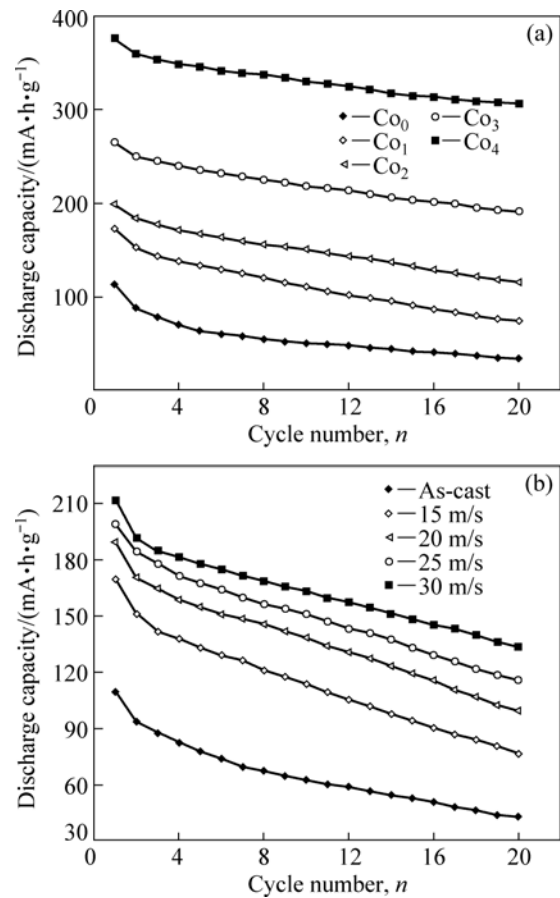


**Fig.7** Evolution of discharge capacity of alloys with cycle number: (a) Effect of Co content with constant spinning rate of 25 m/s; (b) Effect of spinning rate with constant Co content of 2%

The discharge capacity enhanced by Co substitution is ascribed to the increased glass forming ability by Co substitution owing to amorphous  $Mg_2Ni$  alloy showing a large discharge capacity. Fig.7(b) shows that the melt spinning markedly enhances the discharge capacity of the alloys. When the spinning rate is increased from 0 to 30 m/s, the discharge capacity of the  $Co_2$  alloy elevates from 109.9 to 211.4 mA·h/g. The nanocrystalline and amorphous microstructures formed by melt spinning is extremely helpful for enhancing hydrogen diffusivity and solubility, thus it seems to be self-evident that the discharge capacity of the alloys increases with rising spinning rate.

The capacity retaining rate ( $R_h$ ), which is introduced to evaluate accurately the cycle stability of the alloy, is defined as  $R_h = C_n / C_{max} \times 100\%$ , where  $C_{max}$  is the maximum discharge capacity and  $C_n$  is the discharge capacity of the  $n$ th charge-discharge cycle, respectively. According to the above mentioned definition, it can be known that the larger the capacity retaining rate ( $R_h$ ), the better the cycle stability of the alloy.

The capacity retaining rates of the as-cast and spun alloys as function of the cycle number are illustrated in Fig.8. It is shown that the substitution of Co for Ni

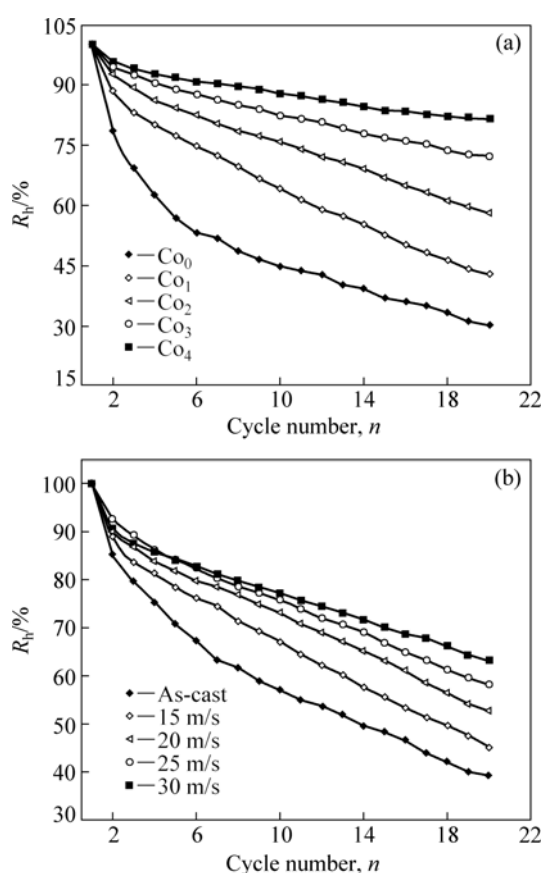


**Fig.8** Evolution of capacity retaining rate of alloys with cycle number: (a) Effect of Co content with constant spinning rate of 25 m/s; (b) Effect of spinning rate with constant Co content of 2%

significantly improves the cycle stability of the as-spun alloy. When Co content increases from 0 to 4%, the capacity retaining rate of as-spun (25 m/s) alloy at 20th cycle rises from 30.42% to 81.51%. The positive impact of Co substitution on the cycle stability of the alloy is ascribed to the glass forming ability enhanced by Co substitution because an amorphous phase improves not only anti-pulverization ability but also anti-corrosion and anti-oxidation abilities of the alloy electrode in a corrosive electrolyte[15–16]. It can be derived from Fig.8(b) that the melt-spinning significantly strengthens the cycle stability of  $Co_2$  alloy. When spinning rate increases from 0 to 30 m/s, the capacity retaining rate of the  $Co_2$  alloys at 20th cycle rises from 39.23% to 63.19%, for which the glass forming ability enhanced by Co substitution is mainly responsible. Based on the above-mentioned results, it can be concluded that an impactful approach for improving the cycle stability of the Mg-based alloy electrodes is to intensify its anti-corrosion and anti-oxidation capabilities.

## 4 Conclusions

1) The investigation on the structures of the as-cast and spun  $Mg_{20}Ni_{10-x}Co_x$  ( $x=0, 1, 2, 3, 4, \%$ , mass fraction) alloys shows that the substitution of Co for Ni significantly enhances the glass forming ability of  $Mg_2Ni$ -type alloy and leads to the refinement of the grains of the as-cast alloy. The substitution of Co for Ni does not change the major phase of  $Mg_2Ni$  in the alloy, but it causes the formation of the secondary phase  $MgCo_2$ .

2) The substitution of Co for Ni in suitable amount significantly improves the hydriding and dehydriding characteristics of the alloy. In addition, it clearly ameliorates the electrochemical performances of the  $Mg_2Ni$ -type alloy, including the discharge capacity and the cycle stability, which is attributed to the glass forming ability enhanced by Co substitution.

3) Melt spinning significantly meliorates the hydriding and dehydriding properties of the alloys, and it markedly enhances the discharge capacity and cycle stability of the alloy containing Co, which is mainly attributed to the formation of the nanocrystalline and amorphous structure produced by melt spinning.

## References

- [1] WOO J H, LEE K S. Electrode characteristics of nanostructured  $Mg_2Ni$ -type alloys prepared by mechanical alloying [J]. J Electrochem Soc, 1999, 146(3): 819–823.
- [2] LIU F J, SUDA S. Properties and characteristics of fluorinated hydriding alloys [J]. J Alloys Comp, 1995, 231: 742–750.
- [3] LIU Y N, ZHANG X J. Effect of lanthanum additions on electrode properties of  $Mg_2Ni$  [J]. J Alloys Comp, 1998, 276: 231–234.

- [4] LEI Y Q, WU Y M, YANG Q M, WU J, WANG Q D. Electrochemical behavior of some mechanic alloyed Mg-Ni-based amorphous hydrogen storage alloys [J]. *Z Phys Chem Bd*, 1994, 183: 379–384.
- [5] IWAKURA C, NOHARA S, INOUE H, FUKUMOTO Y. Surface modification of MgNi alloy with graphite by ball-milling for use in nickel-metal hydride batteries [J]. *Chem Commun*, 1996, 15: 1831–1832.
- [6] KOHNO T, KANDA M. Effect of partial substitution on hydrogen storage properties of Mg<sub>2</sub>Ni alloy [J]. *J Electrochem Soc*, 1997, 144: 2384–2388.
- [7] NOHARA S, FUJITA N, ZHANG S G, INOUE H, IWAKURA C. Electrochemical characteristics of a homogeneous amorphous alloy prepared by ball-milling Mg<sub>2</sub>Ni with Ni [J]. *J Alloys Comp*, 1998, 267: 76–78.
- [8] KIMURA H, MASUMOTO T. Mechanisms for fracture and fatigue-crack propagation in a bulk metallic glass [J]. *Scripta Metall*, 1975, 9: 211–222.
- [9] HUANG L J, LIANG G Y, SUN Z B, WU D C. Electrode properties of melt-spun Mg-Ni-Nd amorphous alloys [J]. *J Power Sources*, 2006, 160: 684–687.
- [10] CHEN H S. Thermodynamic considerations on the formation and stability of metallic glasses [J]. *Acta Met*, 1974, 22(12): 1505–1511.
- [11] SPASSOV T, SOLSONA P, SURIÑACH S, BARÓ M D. Optimization of the ball-milling and heat treatment parameters for synthesis of amorphous and nanocrystalline Mg<sub>2</sub>Ni-based alloys [J]. *J Alloys Comp*, 2003, 349: 242–254.
- [12] ORIMO S, FUJII H. Materials science of Mg-Ni-based new hydrides [J]. *Appl Phys A*, 2001, 72: 167–186.
- [13] WOO J H, LEE K S. Electrode characteristics of nanostructured Mg<sub>2</sub>Ni-type alloys prepared by mechanical alloying [J]. *J Electrochem Soc*, 1999, 146: 819–823.
- [14] TAKAHASHI Y, YUKAWA H, MORINAGA M. Alloying effects on the electronic structure of Mg<sub>2</sub>Ni intermetallic hydride [J]. *J Alloys Comp*, 1996, 242: 98–107.
- [15] ZHANG Y H, LI B W, REN H P, CAI Y, DONG X P, WANG X L. Investigation on structures and electrochemical performances of the as-cast and quenched La<sub>0.7</sub>Mg<sub>0.3</sub>Co<sub>0.45</sub>Ni<sub>2.55-x</sub>Fe<sub>x</sub> (x=0–0.4) electrode alloys [J]. *Int J Hydrogen Energy*, 2007, 32: 4627–4634.
- [16] ZHANG Y H, ZHAO D L, LI B W, REN H P, DONG X P, WANG X L. Investigation on the cycle stability of La<sub>0.7</sub>Mg<sub>0.3</sub>Ni<sub>2.55-x</sub>Co<sub>0.45</sub>Cu<sub>x</sub> (x=0–0.4) electrode alloys [J]. *Trans Nonferrous Met Soc China*, 2007, 17(4): 816–822.

(Edited by YANG Bing)